Empirical equations for estimating the variance of radiation fluctuations in divergent laser beams in snowfalls

N.A. Vostretsov and A.F. Zhukov

Institute of Atmospheric Optics,
Siberian Branch of the Russian Academy of Sciences, Tomsk

Empirical equations are proposed for estimating the variance of radiation fluctuations in divergent laser beams in snowfalls with allowance for the path length, scattering coefficient, detector diameter, and the beam divergence.

Introduction

Laser beam fluctuations in snowfalls are determined by the joint effect of the atmospheric turbulence σ_t^2 and snowflakes σ_s^2. This paper addresses the variance σ^2 caused by the joint effect of turbulence and precipitation.

1. Measurement technique and results

The detailed information about our experiments can be found in our earlier papers, for example, in Ref. 1. In this paper, we concern only the measurement data themselves. We used a narrow divergent beam (NDB) from He−Ne ($\lambda = 0.63 \ \mu$m) lasers of LG-38A and LGN-215 types. The initial radius of the beam α_0, measured at the $1/e$ level, was no larger than 3 mm, and the full divergence angle θ amounted to 10^{-3} rad. We will distinguish a straight path (without reflections from plane mirrors) and a "broken" path (the path with reflections from plane mirrors). The measurements in a NDB were carried out in 80 snowfalls on straight paths with $L = 37$, 130, and 964 m and on broken paths with $L = 130n$, where $n = 2–7$ is the number of reflections from plane mirrors. The detector diameter D was equal to 0.5, 0.3, or 0.1 mm (in the most cases $D = 0.1$ mm). The total detector field of view γ was $2.7 \cdot 10^{-2}$ rad. We calculated the relative variance $\sigma^2 = <(U - <U>)^2>/<U>^2$, where U is the signal at the output of a linear amplifier, whose input is the signal from the photodetector; angular brackets < > denote time averaging. The averaging time was about 20 s. According to our estimates, the measurement error of σ^2 in the variability range from 0.01 to 1.0 did not exceed 15%. Earlier in Refs. 2−4, three modes were separated in NDB radiation fluctuations with the increase of the optical depth τ of the propagation path. The variance σ^2 and the level of σ first increase, saturate, and then decrease. From here on, we will call them the first, second, and third modes, respectively. In Refs. 2−4 it was found that, in NDB in the first and second fluctuation modes, σ^2 increases with the increase of the maximum size of snowflakes D_m. Such a behavior of fluctuations was predicted in

Ref. 5. For NDB it was established in Ref. 4 that the variance of fluctuations decreases with the increase of the detector diameter in the first two modes. The particle size distribution was not measured, but only the maximum particle size D_m was estimated. The measured values of the variance σ^2 were classified in relation to the optical depth τ and the maximum size of snowflakes D_m.

Figure 1 depicts the variance measured in NDB along the 964 m long path. It should be emphasized that these data were obtained on the straight path without reflections from plain mirrors.

At the optical depth $\tau \leq 4.5$, the variance was measured using a detector with $D = 0.1$ mm. The signal-to-noise ratio S/N was no lower than 20. At $\tau \geq 4.5$, to improve the S/N, the detector diameter was increased to 0.5 mm. The variance was measured in 23 snowfalls, and 1800 values of the variance were obtained. Only some of them are shown in Fig. 1. In the first and second modes, a considerable fraction of measured variance values coincide with the values shown in Fig. 1. This coincidence is especially frequent in the first mode. We can clearly see from Fig. 1 that the variance values measured at the close values of the optical depth differ widely. We believe, as before, that these differences are caused by the significant difference in the snowflake size. It follows from Fig. 1 that the maximum value of the variance in coarse snowflakes is close to unity. It is not an instrumental effect, because in sheeted snow, when $D_m \approx 7$ mm, the average variance[4] achieved the value ≈ 2.2 and saturated at the level ≈ 1.2 at $\tau = 2–3$. The variance higher than unity was measured by the same variance meter on the path 964 m long in NDB without precipitation (under fine weather conditions).

In Ref. 4, the mean values of the level $\bar{\sigma}$ at $\tau \leq 4.5$ were determined from all measurements without the consideration of sheeted snow with $D = 0.1$ mm for NDB and the relationship connecting $\bar{\sigma}$ and τ was proposed. Here we transform this relationship for the variance. Finally, we have

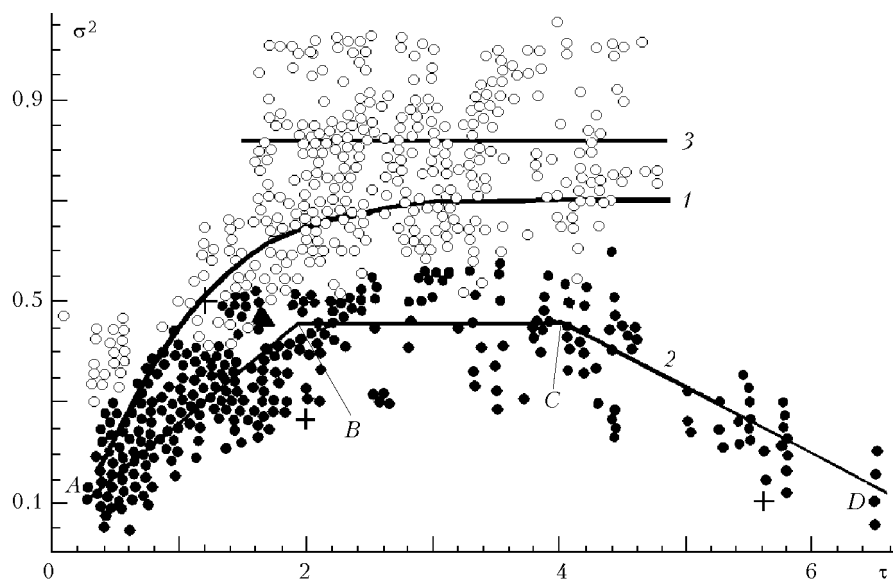$$\overline{\sigma}^2(\tau) \cong 0.7 \left[1 - \exp(-1.65\tau)\right]^2. \qquad (1)$$

Fig. 1. Variance σ^2 as a function of the optical depth τ: $D_m < 5$ mm (●); $D_m \geq 5$ mm (○); $L = 964$ m.

This equation corresponds to curve *1* in Fig. 1. It should be emphasized that Eq. (1) approximates the variance measured in NDB along 11 paths in 80 snowfalls, including broken paths. Curve *1* (Fig. 1) poorly describes individual measurements. Real values may have twice as different values, for example, at $\tau \approx 2$. It is logical to look for the better approximation of experimental results. For this purpose, all measurements should be divided into two categories in accordance with the maximum size of snowflakes. Snowfalls with $D_m < 5$ mm will be referred to as finely dispersed and those with $D_m \geq 5$ mm will be referred to as coarsely dispersed. In finely dispersed snowfalls, the three modes of fluctuations, which were mentioned above, are clearly seen.

The physical processes determining the existence of the three different modes of fluctuations are described in Ref. 5. The increase of the variance in the first mode is caused by the increase in number of snowflakes, the saturation in the second mode is determined by the mutual screening among particles (as was noted, for the first time, in Ref. 6), and the decrease of the variance in the third mode is a consequence of the increasing role of the slightly fluctuating refracted radiation in the average signal.[3] Fluctuations of the detected signal are determined, in the first turn, by the motion of snowflakes.[7]

In each mode, the dependence of the variance on the optical depth in finely dispersed snowfalls is approximated by the broken line *2* (see Fig. 1). The boundaries of the second mode in finely dispersed snowfalls can be determined from the value of saturation ($\sigma^2_{sat} \approx 0.45$) and the error of variance measurements. The lower and upper boundaries of the second mode in finely dispersed snowfalls can be found from the broken line *2* at those values of the optical depth, at which the variance values differ by 30% (2 × 15) from the saturated value σ^2_{sat}, that is,

the boundary value σ^2_b is approximately equal to 0.30. In this case, the lower boundary of the second mode is achieved at $\tau \approx 1.2$, while the upper one at $\tau \approx 5.1$.

The equations describing the dependence $\sigma^2(\tau) = f(\tau)$ in each mode have the form:

mode 1 (straight line *AB*)

$$\sigma^2(\tau) = 0.06 + 0.2\tau \quad \text{at } 0.2 \leq \tau \leq 1.9, \qquad (2)$$

mode 2 (straight line *BC*)

$$\sigma^2(\tau) \cong 0.45 \qquad \text{at } 1.9 \leq \tau \leq 4.0, \qquad (3)$$

mode 3 (straight line *CD*)

$$\sigma^2(\tau) = 1.0 - 0.13\tau \text{ at } 4.0 \leq \tau \leq 6.5. \qquad (4)$$

The maximum relative error in description of the experimental results by the straight line *AB* is no higher than 40, for *BC* it is no higher than 70, and for *CD* it is no higher than 120%. The measured variance values having maximum errors in the case of representing the dependence by the broken line are marked by crosses. The maximum error was calculated as $(|x_2 - x_1|/x_1) \cdot 100\%$, where x_1 is the measured variance, x_2 is the variance calculated by Eqs. (2)–(4).

The variance in coarsely dispersed snowfalls in the second (saturation) mode is approximated by the straight line *3* (see Fig. 1):

$$\sigma^2 \cong 0.80 \text{ at } 1.6 \leq \tau \leq 4.8, \qquad (5)$$

which is in a close agreement with the results from Ref. 2. The maximum relative error, calculated as before, is no higher than 80% for the variance value marked by triangle near letter *B*.

2. Variance σ^2 as a function of the beam divergence angle θ

The measurements in divergent beams with the increase of the divergence angle were carried out only

in the first mode and in finely dispersed snowfalls. Figure 2 shows the dependence of the variance σ^2 on the logarithm of the divergence angle θ of a narrow laser beam in finely dispersed snowfalls. In these measurements, $\tau \approx 0.1$, $L = 130$ m, $D_{\mathrm{m}} = 1-3$ mm, and $\theta = 10^{-3} - 8.3 \cdot 10^{-2}$. The digits indicate the number of snowfalls, in which the measurements have been conducted. At all θ, in every snowfall, no less than ten measurements of the variance have been carried out. The vertical bars show the range of σ^2 variations in all the measurements, and the dots show the average values. The divergence of the He–Ne laser beam was changed by the use of replaceable lenses with different focal lengths, which were set on the beam axis. The left point in Fig. 2 corresponds to NDB. The average variance increases linearly as $\ln \theta$ increases in the range $-7 \leq \ln \theta \leq -2.5$, which is described by the following dependence:

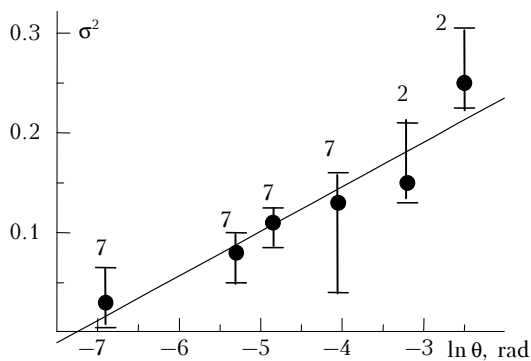$$\bar{\sigma}^2 = 0.30 + 0.04 \ln \theta. \qquad (6)$$

Fig. 2. Variance σ^2 as a function of the beam divergence angle θ; $L = 130$ m. Digits 7 and 2 indicate the number of snowfalls.

The increase of $\bar{\sigma}^2$ with growing θ will likely stop, when the laser beam will be close to a spherical wave.

3. Averaging effect of the receiving aperture

The effect of the detector diameter on the variance can be estimated with the aid of the averaging function[8]:

$$G(R) = \{<P^2>/<P>^2 - 1\}\{<I^2>/<I>^2 - 1\}^{-1} = \sigma_P^2/\sigma_I^2,$$

which shows, how many times σ_P^2 (the relative variance of fluctuations of the flux P passed through the aperture of the radius R ($D = 2R$)) is smaller than σ_I^2 (the relative variance of intensity fluctuations of the detected wave, that is, when $R \ll R_{\mathrm{c}}$, where R_{c} is the spatial radius of correlation of intensity fluctuations). Since $D = 0.1$ mm, we measure intensity fluctuations, because the measurements are conducted in the first mode, when R_{c} is approximately equal to $D_{\mathrm{m}}/2$ (Ref. 4).

The average value of the function $\bar{G}$ decreases linearly with the increase of $\ln D$. Let us emphasize

that the function $G(D/2)$ is obtained from the measurements along the broken path with $L = 260 = (130 \times 2)$ m in finely dispersed snowfalls.[4] The straight line in Fig. 3 corresponds to the equation

$$\bar{G}(D/2) = 0.6 - 0.15 \ln D, \qquad (7)$$
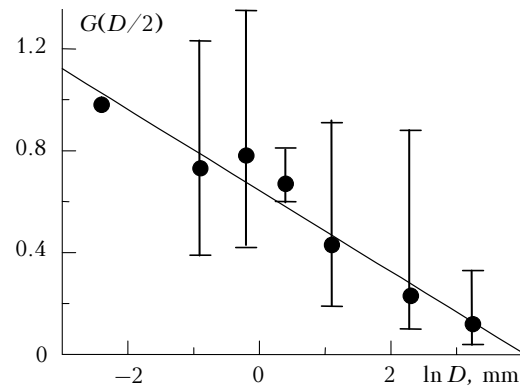
when $-2.3 \leq \ln D \leq 3.2$ mm.

Fig. 3. Averaging function of the receiving aperture: $L = 260$ m; $D_{\mathrm{m}} = 1-3$ mm; $\tau \approx 0.1-0.5$.

As would be expected, the measured variance $\bar{\sigma}^2$ decreases with the increase of the detector diameter:

$$\bar{\sigma}^2 = \sigma_{0.1}^2 \, \bar{G}(D/2). \qquad (8)$$

4. Estimation of variance from the meteorological visual range

The meteorological visual range S_{m} is usually used in practice to characterize the optical conditions in the atmosphere. We will assume below that the path length L is known exactly. Knowing S_{m}, it is easy to find the volume scattering coefficient α (km^{-1}) for the visible radiation as $\alpha = 3.9/S_{\mathrm{m}}$ and the optical depth by formula $\tau = \alpha L$. Having known L and α (or S_{m}), the variance for the fine snow ($D_{\mathrm{m}} < 5$ mm), $D = 0.1$ mm and the optical depth $\tau \leq 0.6$ (first mode) can be estimated by the equation obtained in Ref. 9:

$$\sigma^2 \approx 0.3 L \alpha \approx 1.2 L / S_{\mathrm{m}}. \qquad (9)$$

Equation (9) is true for NDB at $L = 14-964$ m and the conditions mentioned above. Then, according to Ref. 9, the maximum relative error with the use of Eq. (9) does not exceed 40%.

5. Examples of variance estimation

The variance σ^2 can be estimated by Eqs. (1)–(9). The estimate of σ^2 can be useful in a laser beam guidance of a guided missile to a target in snowfalls.[10] It should be emphasized that of primary significance in snowfalls is the extinction of a laser beam, while its fluctuations, though being always present, are much lower than maximum turbulent fluctuations[1] and

decrease considerably with the increase of the detector diameter. It follows from the above-said that to estimate σ^2, it is necessary to know D_m and τ. It is proposed to estimate S_m rather than τ from visual observations in daytime and from atmospheric transmittance in nighttime.

Let us present some examples of σ^2 estimated for divergent beams in some particular cases. Let $S_m = 1$ km, $L = 1$ km, $D = 0.1$ mm, $\theta = 10^{-3}$ rad, $D_m < 5$ mm, that is, the snow is finely dispersed. Then $\alpha = 3.9$ km^{-1} ($\tau \approx 3.9$), and the second mode takes place, in which $\sigma^2 \approx 0.45$. At $S_m = 0.5$ km and the same L, D, θ, and D_m ($\tau \approx 8$), the third mode takes place, which at $\tau \approx 8$ is characterized by the low value of σ^2 ($\sigma^2 \leq 0.1$). If $S_m \approx 3$ km and L, D, θ, and D_m are the same, then $\alpha \approx 1.3$ km^{-1} ($\tau \approx 1.3$), that is, the first mode takes place. Then we can use Eq. (2), according to which $\sigma^2 \approx 0.3$. If $S_m \approx 7$ km, then $\alpha \approx 0.5$ km^{-1} ($\tau \approx 0.5$). Then from Eq. (2) $\sigma^2 \approx 0.16$, and from Eq. (9) $\sigma^2 \approx 0.17$. So the values of σ^2 estimated by Eqs. (2) and (9) are quite close. In the case of coarse snow ($D_m \geq 5$ mm), σ^2 can be estimated only in the second mode by Eq. (5). Emphasize that the effects of the divergence angle of a narrow laser beam and the detector diameter have been studied at very small values of the optical depth.

Then estimate the effect of the beam divergence angle. Let $\tau \approx 0.5$, then from Eq. (2) we obtain $\sigma^2 \approx 0.16$. With the increase of the beam divergence, the variance increases, for example, at $\ln \theta = -4$ ($\theta = 1.85 \cdot 10^{-2}$ rad) the variance increases by 4.7 times with respect to NDB according to Eq. (6), that is, $\sigma^2 \approx 0.75$.

With the increase of the detector diameter, the variance increases and at $\ln D = 2.3$ ($D = 10$ mm) according to Eq. (7) $G(D/2) = 0.27$. In accordance with Eq. (8), we obtain $\sigma^2 = 0.85 \times 0.27 = 0.20$. Just this is the estimate of the variance in finely dispersed snowfall at $\tau \approx 0.5$, $\theta = 1.8 \cdot 10^{-2}$ rad, and $D = 10$ mm.

Conclusions

On a straight path about 1 km long with a small-diameter detector, we have obtained the empirical equations suitable for estimating the variance in NDB in finely dispersed snowfalls as a function of the optical depth in three modes, as well as the empirical equation for the variance in coarsely dispersed snowfalls as a function of D_m in the saturation mode. The effect of the maximum size of snowflakes on the variance in NDB can be weaker, if the initial diameter of the beam is taken greater than the size of the snowflakes. The increase of the variance with the increasing beam divergence has been found experimentally for the first time at the low values of the optical depth. It may prove untrue if the atmosphere is increasingly turbid due to snow, so this dependence should not be used automatically at the high atmospheric turbidity without the appropriate experimental data.

The decrease of the variance with the increase in the detector diameter has been obtained at the low values of the optical depth. With the increase of the optical depth, the aperture effect will also take place. But the quantitative equation for it will be different from that presented in this paper, because it is expected from theoretical reasoning that the spatial correlation radius of the intensity will decrease with the increasing optical depth.

References

1. A.F. Zhukov and N.A. Vostretsov, Atmos. Oceanic Opt. **16**, No. 12, 996–1048 (2003).
2. A.F. Zhukov, Atmos. Oceanic Opt. **6**, No. 1, 19–21 (1993).
3. A.G. Borovoi, N.A. Vostretsov, A.F. Zhukov, B.A. Kargin, and S.M. Prigarin, Atmos. Oceanic Opt. **10**, No. 3, 141–145 (1997).
4. A.F. Zhukov and N.A. Vostretsov, Atmos. Oceanic Opt. **9**, No. 8, 670–676 (1996).
5. A.G. Borovoi, Izv. Vyssh. Uchebn. Zaved., Radiofiz. **25**, No. 4, 391–409 (1982).
6. M.V. Kabanov, Yu.A. Pkhalagov, and V.E. Gologuzov, Izv. Akad. Nauk SSSR, Fiz. Atmos. Okeana **7**, No. 7, 804–807 (1971).
7. V.E. Zuev and M.V. Kabanov, *Optical Signal Transfer through the Earth's Atmosphere (under Noise Conditions)* (Sov. Radio, Moscow, 1977), 368 pp.
8. A.S. Gurvich, A.I. Kon, V.L. Mironov, and S.S. Khmelevtsov, *Laser Radiation in the Turbulent Atmosphere* (Nauka, Moscow, 1976), 277 pp.
9. N.A. Vostretsov and A.F. Zhukov, Atmos. Oceanic Opt. **16**, No. 1, 35–37 (2003).
10. A.G. Shipunov and E.N. Semashin, *Optical Communication Lines of Small-Sized Guided Missiles under the Conditions of Noise from Propulsion Systems* (TSC Informatika, Moscow, 2000), 180 pp.